IOPscience iopscience.iop.org

Home Search Collections Journals About Contact us My IOPscience

Modification of the gapless state in non-uniform semiconductor alloys

This article has been downloaded from IOPscience. Please scroll down to see the full text article.

2000 J. Phys.: Condens. Matter 12 4141

(http://iopscience.iop.org/0953-8984/12/17/317)

View the table of contents for this issue, or go to the journal homepage for more

Download details:
IP Address: 171.66.16.221
The article was downloaded on 16/05/2010 at 04:52

Please note that terms and conditions apply.

J. Phys.: Condens. Matter **12** (2000) 4141–4149. Printed in the UK PII: S0953-8984(00)08386-7

Modification of the gapless state in non-uniform semiconductor alloys

M V Strikha and F T Vasko

Institute of Semiconductor Physics, NAS of Ukraine, Kyiv, 252650, Ukraine

Received 4 September 1999, in final form 18 February 2000

Abstract. Semiconductor alloy with spatially non-uniform change of composition close to the averaged value, corresponding to the transition between gapless and narrow-gap states, is studied. The density of states is calculated within the two-band model of band structure with random change of the position of the conduction band bottom and with a uniform valence band top. The appearance of an inhomogeneity-induced gap in the energy dependence of the density of states is discussed for the cases of short-range and long-range non-uniformities of composition. The peculiarities of the kinetic effects due to modification of the gapless state in such non-uniform semiconductors are discussed.

1. Introduction

The peculiarities of the kinetic and optical properties of gapless semiconductor alloys were studied in detail [1, 2] within the 'virtual'-crystal model. In the framework of this model the $\boldsymbol{k}\cdot\boldsymbol{p}$ Hamiltonian parameters depend on alloy composition, but the model does not take into consideration the non-uniformities of composition for the range of distances of the order of the lattice constant, a. To the best of our knowledge, such non-uniformities have only been discussed for finite-gap alloys [3, 4]. The band structure of several gapless semiconductors was calculated in [5] throughout the whole concentration range from semimetal to finite gap. However, there was no special emphasis placed on the region where the gap opens.

The transition between the gapless and narrow-gap states of the energy spectrum occurs with the change of alloy composition, i.e. the change of x_r for alloys such as $A_xA'_{1-x}B$ (e.g. $Pb_xSn_{1-x}Te$ or $Hg_xCd_{1-x}Te$) in the vicinity of $x = x_c$. Due to the smooth (i.e. slowly changing at distances of the order of a) non-uniformities of composition in these alloys, the critical value of the composition, x_c, is realized at the transition point only as an average, $x_c = \langle x_r \rangle$ ($\langle \cdots \rangle$ means the average over the spatial non-uniformities of the composition). Therefore, consideration of this non-uniformity indicates the gapless semiconductor to be of type-I structure (like α-Sn, HgTe or HgSe, and alloys based on lead chalcogenide), with random domains with positive and negative gaps, separated by inversion heterojunctions as shown in figure 1. (In the opposite case of gapless semiconductors of type II, like HgCdTe alloys, a structure with gapless and narrow-gap domains occurs, because heavy-hole bands exist then, and their positions change only slightly with the alloy composition.)

The averaging over these random non-uniformities in type-I gapless semiconductors results in the appearance of an effective gap in the energy dependence of the density of states, $\rho(E)$. Such effective gaps are determined both by average gap variance $\Delta\varepsilon_g = (\mathrm{d}\epsilon_g/\mathrm{d}x)\,\overline{\Delta x}$ (here $\overline{\Delta x}$ is the average variance of the composition from x_c and the derivative $(\mathrm{d}\epsilon_g/\mathrm{d}x)$ is

 © 2000 IOP Publishing Ltd

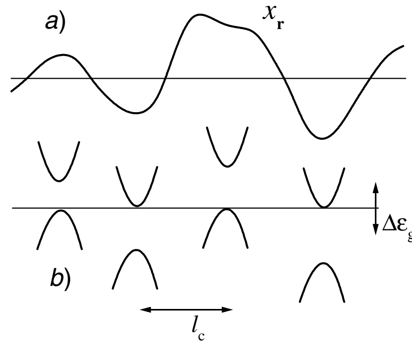

Figure 1. The spatial change of the ±-band extrema $E_\pm$ (l_c: correlation length; $\Delta\varepsilon_g$: gap-width variance).

taken at $x \simeq x_c$) and correlation length l_c. This modification of the ideal density of states $\rho_0(E) = E^2/\pi^2(\hbar s)^3$ which is obtained for the linear spectrum $\pm s|\boldsymbol{p}|$ of electrons (+) and holes (−) (s is the interband velocity and $\boldsymbol{p}$ is the momentum) leads to the change of kinetic phenomena in non-uniform gapless semiconductors. These changes of the density of states and interband absorption can be obtained from the phenomenological averaging of the expressions for the narrow-gap material over the long-range inhomogeneities with gap ϵ_g near $\langle\epsilon_g\rangle = 0$ (see the appendix).

In this paper we present microscopic calculations of $\rho(E)$ within the two-band model of band structure with isotropic bands. The main assumption of the analytic examination made here is the use of the band diagram of the alloy with the plane valence band (see the scheme for the random spatial change of the conduction and valence band extrema in figure 1). On the assumption of a fixed valence band top, the matrix (which is 4×4 due to the spin) Green's function is given through the path integral for a particle with a quadratic dispersion law and the effective mass $m^* = \Delta\varepsilon_g/2s^2$ in the random potential $E(x_r - x_c)/\overline{\Delta x}$. The calculation of $\rho(E)$ is reduced thus to the averaging of this integral, performed here for the cases of short-range and long-range non-uniformities of the composition.

Below, in section 2, the one-particle matrix Green's function is calculated and the density of states is expressed through this function. Further on, the energy dependences of the density of states for the cases of long-range (section 3) and short-range (section 4) non-uniformities of the composition are discussed. In the concluding section we present the numerical estimations and discuss the approximations being used.

2. Green's functions

Neglecting the contribution of the remotely spaced bands, we use a Hamiltonian that is linear in the momentum operator, $\hat{\boldsymbol{p}}$. Therefore the matrix Green's function $\hat{G}_\varepsilon(\boldsymbol{r}, \boldsymbol{r}')$ is introduced by the equation

$$\left[\hat{\mathbf{v}}\hat{\boldsymbol{p}} + \hat{\epsilon}_r - \varepsilon\right]\hat{G}_\varepsilon(\boldsymbol{r}, \boldsymbol{r}') = \delta(\boldsymbol{r} - \boldsymbol{r}'). \tag{1}$$

Here the interband velocity matrix, $\hat{\mathbf{v}}$, is assumed to be independent of the alloy composition while the spatial dependences of the conduction and valence band extrema are determined by the diagonal matrix $\hat{\epsilon}_r$. The two-band model of the gapless semiconductor of type I with fixed valence band extrema is described by

$$\hat{\mathbf{v}} = s\hat{\boldsymbol{\sigma}}\hat{\boldsymbol{\rho}}_1 \qquad \hat{\epsilon}_r = \Delta\varepsilon_g\,\delta(\boldsymbol{r})(1 + \hat{\rho}_3)/2. \tag{2}$$

The velocity s in equation (2) determines the band spectrum of the uniform gapless semiconductor $\pm s|\boldsymbol{p}|$, $\hat{\boldsymbol{\sigma}}$ is the Pauli matrix, and $\hat{\boldsymbol{\rho}}_{1,2,3}$ are the 2×2 matrices introduced in [6]. These matrices operate on the band states. In the expression for $\hat{\boldsymbol{\epsilon}}_r$ we use the linear dependence between the average variance of the composition $\Delta\overline{x}$ and the average variance of the gap width $\Delta\varepsilon_g$; $\delta(\boldsymbol{r}) = (x_r - x_c)/\overline{\Delta x}$ is a random function with $\langle\delta(\boldsymbol{r})^2\rangle = 1$. We consider the case of Gaussian correlation of the non-uniformities:

$$\langle\delta(\boldsymbol{r})\delta(\boldsymbol{r}')\rangle \equiv W(|\boldsymbol{r}-\boldsymbol{r}'|) = \exp(-|\boldsymbol{r}-\boldsymbol{r}'|^2/l_c^2)$$

for the numerical estimations below.

It is convenient to rewrite equation (1) using the band quantum numbers $j = c, v$ (for conduction and valence) and the system of four equations for the spin-dependent matrices. $\hat{G}_\varepsilon^{j,j'}(\boldsymbol{r},\boldsymbol{r}')$ now takes the form

$$\begin{bmatrix} \Delta\epsilon_g\,\delta(\boldsymbol{r}) - \varepsilon & s(\hat{\boldsymbol{\sigma}}\hat{\boldsymbol{p}}) \\ s(\hat{\boldsymbol{\sigma}}\hat{\boldsymbol{p}}) & -\varepsilon \end{bmatrix} \hat{G}_\varepsilon^{jj'}(\boldsymbol{r},\boldsymbol{r}') = \delta(\boldsymbol{r}-\boldsymbol{r}')\delta_{jj'}. \tag{3}$$

For the approximation of the fixed valence band we can exclude the matrices $\hat{G}_\varepsilon^{vc}$, $\hat{G}_\varepsilon^{vv}$ from the lower pair of equations in this system through the equalities

$$\begin{aligned} \hat{G}_\varepsilon^{vc}(\boldsymbol{r},\boldsymbol{r}') &= \frac{s}{\varepsilon}(\hat{\boldsymbol{\sigma}}\hat{\boldsymbol{p}})\hat{G}_\varepsilon^{cc}(\boldsymbol{r},\boldsymbol{r}') \\ \hat{G}_\varepsilon^{vv}(\boldsymbol{r},\boldsymbol{r}') &= \frac{s}{\varepsilon}(\hat{\boldsymbol{\sigma}}\hat{\boldsymbol{p}})\hat{G}_\varepsilon^{cv}(\boldsymbol{r},\boldsymbol{r}') - \frac{\delta(\boldsymbol{r}-\boldsymbol{r}')}{\varepsilon}. \end{aligned} \tag{4}$$

Therefore, independent equations of second order are obtained for the retarded Green's functions $\hat{G}_\varepsilon^{cc}$, and $\hat{G}_\varepsilon^{cv}$:

$$\begin{aligned} \left[\frac{\hat{\boldsymbol{p}}^2}{2m^*} + E\delta(\boldsymbol{r}) - \frac{E^2}{\Delta\epsilon_g} - \mathrm{i}\lambda(\operatorname{sgn} E)\right]\hat{G}_E^{cc}(\boldsymbol{r},\boldsymbol{r}') &= \frac{E}{\Delta\varepsilon_g}\delta(\boldsymbol{r}-\boldsymbol{r}') \\ \left[\frac{\hat{\boldsymbol{p}}^2}{2m^*} + E\delta(\boldsymbol{r}) - \frac{E^2}{\Delta\varepsilon_g} - \mathrm{i}\lambda(\operatorname{sgn} E)\right]\hat{G}_E^{cv}(\boldsymbol{r},\boldsymbol{r}') &= \frac{s(\hat{\boldsymbol{\sigma}}\hat{\boldsymbol{p}})}{\Delta\epsilon_g}\delta(\boldsymbol{r}-\boldsymbol{r}') \end{aligned} \tag{5}$$

where $\varepsilon = E - \mathrm{i}\lambda$ and $\lambda \to +0$.

The solutions of these equations can be written in terms of path integrals in analogy with [7] (below we use $\hbar = 1$ in the intermediate expressions, for reasons of convenience):

$$G_t(\boldsymbol{r},\boldsymbol{r}') = \mathrm{i}\int_{\boldsymbol{x}_0=\boldsymbol{r}'}^{\boldsymbol{x}_t=\boldsymbol{r}} \mathcal{D}\{\boldsymbol{x}_\tau\}\exp\left\{-\mathrm{i}\int_0^t \mathrm{d}\tau\left[\frac{m^*}{2}\dot{\boldsymbol{x}}_\tau^2 - E\delta(\boldsymbol{x}_\tau)\right]\right\}. \tag{6}$$

The components of $\hat{G}_E^{jj'}$ for positive or negative energies E are expressed through the function

$$K_E(\boldsymbol{r},\boldsymbol{r}') = \begin{cases} \displaystyle\int_{-\infty}^0 \mathrm{d}t\,\exp(\lambda t - \mathrm{i}E^2 t/\Delta\varepsilon_g)G_t(\boldsymbol{r},\boldsymbol{r}') & E > 0 \\ \displaystyle\int_0^\infty \mathrm{d}t\,\exp(-\lambda t - \mathrm{i}E^2 t/\Delta\varepsilon_g)G_t(\boldsymbol{r},\boldsymbol{r}') & E < 0\,. \end{cases} \tag{7}$$

Here the change of the limits of the integration over time at $E = 0$ is determined by the contribution of $\mathrm{i}(\operatorname{sgn} E)\lambda$ in equation (5). The results take the form

$$\begin{aligned} \hat{G}_E^{cc}(\boldsymbol{r},\boldsymbol{r}') &= -\mathrm{i}\frac{|E|}{\Delta\epsilon_g}K_E(\boldsymbol{r},\boldsymbol{r}') \\ \hat{G}_E^{cv}(\boldsymbol{r},\boldsymbol{r}') &= -\mathrm{i}(\operatorname{sgn} E)\frac{(\hat{\boldsymbol{\sigma}}\hat{\boldsymbol{p}}')}{2m^* s}K_E(\boldsymbol{r},\boldsymbol{r}') \end{aligned} \tag{8}$$

and using equations (4) we obtain

$$\begin{aligned}\hat{G}_E^{vc}(\boldsymbol{r},\boldsymbol{r}') &= -\mathrm{i}(\mathrm{sgn}\,E)\frac{(\hat{\boldsymbol{\sigma}}\hat{\boldsymbol{p}})}{2m^*s}K_E(\boldsymbol{r},\boldsymbol{r}')\\ \hat{G}_E^{vv}(\boldsymbol{r},\boldsymbol{r}') &= -\mathrm{i}\frac{(\hat{\boldsymbol{\sigma}}\hat{\boldsymbol{p}})(\hat{\boldsymbol{\sigma}}\hat{\boldsymbol{p}}')}{2m^*|E|}K_E(\boldsymbol{r},\boldsymbol{r}') - (\mathrm{sgn}\,E)\frac{\delta(\boldsymbol{r}-\boldsymbol{r}')}{|E|}.\end{aligned} \tag{9}$$

Therefore, equations (6)–(9) give the expression for the matrix Green's function with the approximation of a fixed valence band. This enables us to write $\rho(E)$ in terms of the average of these Green's functions. Such an average would differ from the ordinary equations of [8] in considering additional sums over the discrete variables only. The density of states, averaged over the non-uniformity of the composition, is given by the expression

$$\rho(E) = \frac{\mathrm{Im}}{\pi V}\int \mathrm{d}\boldsymbol{r}\;\mathrm{tr}\langle\hat{G}_E(\boldsymbol{r},\boldsymbol{r}')\rangle \tag{10}$$

where 'tr' means the trace over the matrix variables and V is the normalizing volume.

3. The long-range case

In order to calculate the density of states, we substitute the expressions for G_E^{jj} ($j = c, v$), determined from equations (6)–(9), into equation (10). After summation over the spin and taking the average over the composition non-uniformity, we get

$$\rho(E) = \frac{|E|}{\Delta\varepsilon_g} - \frac{\Delta_{\boldsymbol{R}}}{2m^*|E|}\frac{2}{\pi}\mathrm{Re}\begin{cases}\displaystyle\int_{-\infty}^0 \mathrm{d}t\;\mathrm{e}^{\lambda t-\mathrm{i}E^2t/\Delta\epsilon_g}g_t(\boldsymbol{R})|_{\boldsymbol{R}\to0} & E>0\\ \displaystyle\int_0^\infty \mathrm{d}t\;\mathrm{e}^{-\lambda t-\mathrm{i}E^2t/\Delta\varepsilon_g}g_t(\boldsymbol{R})|_{\boldsymbol{R}\to0} & E<0\end{cases} \tag{11}$$

and the averaged path integral $g_t(\boldsymbol{R})$ here depends on $\boldsymbol{R} = \boldsymbol{r} - \boldsymbol{r}'$. Using the well-known result for the average of the random potential in the exponent (see [9] and the appendix below), while calculating the contributions of the random potential energy to the action, we obtain

$$g_t(\boldsymbol{R}) = \int_{\boldsymbol{x}_0=0}^{\boldsymbol{x}_t=\boldsymbol{R}}\mathcal{D}\{\boldsymbol{x}_\tau\}\exp\left[-\mathrm{i}\int_0^t \mathrm{d}\tau\;\frac{m^*}{2}\dot{\boldsymbol{x}}_\tau^2 - \frac{E^2}{2}\int_0^t\mathrm{d}\tau\int_0^t\mathrm{d}\tau'\;W(|\boldsymbol{x}_\tau-\boldsymbol{x}_{\tau'}|)\right]. \tag{12}$$

For the case of long-range non-uniformities, the quasi-classical approximation is valid. Therefore it is convenient to separate the linear path $\boldsymbol{R}\tau/t$ and to rewrite equation (12) in terms of the contour path integral:

$$\begin{aligned}g_t(\boldsymbol{R}) = \exp\left(-\frac{\mathrm{i}m^*\boldsymbol{R}^2}{2t}\right)\oint\mathcal{D}\{\boldsymbol{y}_\tau\}\exp\bigg\{&-\mathrm{i}\int_0^t\mathrm{d}\tau\;\frac{m}{2}\dot{\boldsymbol{y}}_\tau^2\\ &-\frac{E^2}{2}\int_0^t\mathrm{d}\tau\int_0^t\mathrm{d}\tau'\;W\left[\left|\boldsymbol{y}_\tau-\boldsymbol{y}_{\tau'}+\boldsymbol{R}\frac{(\tau-\tau')}{t}\right|\right]\bigg\}.\end{aligned} \tag{13}$$

The main contribution to the path integral of equation (13) is made by the classical path; the variation of the action over this trajectory is zero. This trajectory is determined by the Euler–Lagrange integral–differential equation:

$$m^*\ddot{\boldsymbol{y}}_\tau - \mathrm{i}\frac{E^2}{l_c^2}\int_0^t\mathrm{d}\tau'\left(\boldsymbol{y}_\tau-\boldsymbol{y}_{\tau'}+\boldsymbol{R}\frac{\tau-\tau'}{t}\right)W\left(\left|\boldsymbol{y}_\tau-\boldsymbol{y}_{\tau'}+\boldsymbol{R}\frac{\tau-\tau'}{t}\right|\right) = 0. \tag{14}$$

Further on, we shall use the estimate for the greatest (corresponding to the time $t = \tau/2$) deviation of the classical path from the linear path, chosen above. This estimate can be obtained from equation (14):

$$|y_{max}(t)/l_c| \simeq E^2t^3/8m^*l_c^2. \tag{15}$$

Later, the contributions of such the times t will be essential in the calculation of $\rho(E)$, to make equation (15) small, so that the deviations of the classical path from the linear one can be neglected. In this case the paths $\boldsymbol{y}_\tau$ determine the contribution of the quantum corrections. This contribution can be estimated from the consideration of the second variation of the functional in equation (14). It is small in the parameter of equation (15). Such an inequality permits us to consider the linear paths only, while calculating $\rho(E)$. After the calculation of the path integral in equation (13) we get

$$g_t(\boldsymbol{R}) \simeq \left(\frac{\mathrm{i}m^*}{2\pi t}\right)^{3/2} \exp\left[-\frac{\mathrm{i}m^*\boldsymbol{R}^2}{2t} - \frac{E^2}{2}\int_0^t \mathrm{d}\tau \int_0^t \mathrm{d}\tau'\, W\left(\left|\boldsymbol{R}\frac{\tau-\tau'}{t}\right|\right)\right]. \tag{16}$$

Further on, by substituting $g_t(\boldsymbol{R})$ into equation (11), and with the use of the equality $g_t(\boldsymbol{R}) = g_{-t}(\boldsymbol{R})^*$, we will calculate $\Delta_{\boldsymbol{R}}$ at $\boldsymbol{R} \to 0$ for the second term of equation (11). The contribution of small $\boldsymbol{R}$ in the factor $\exp(-m\boldsymbol{R}^2/2t)$ must be taken into account in the vicinity of the anomaly at $t = 0$. Finally, the dimensionless density of states $\rho(E)/\rho_0$ ($\rho_0 \equiv \Delta\epsilon_g^2/[\pi^2(\hbar s)^3]$ is the density of states of the ideal gapless semiconductor at energy $\Delta\varepsilon_g$) is determined, by analogy with the long-range-limit case for the finite-gap semiconductors [10], in terms of parabolic cylinder functions. The final expression is a function of the dimensionless variable $\epsilon = |E|/\Delta\varepsilon_g$ only:

$$\rho(E)/\rho_0 = \begin{cases} \epsilon^2 - 1/16 + \mathrm{o}(\epsilon^{-2}) & \epsilon \gg 1 \\ \sqrt{\pi/2}\epsilon^3 + \mathrm{o}(\epsilon^5) & \epsilon \ll 1. \end{cases} \tag{17}$$

These asymptotic expansions for the large and small arguments correspond to the phenomenological expressions obtained in the appendix. The expressions for $\rho(E)/\rho_0$ must agree for the region of finite ϵ, and we see that the transition between them occurs at rather small dimensionless energies of the order of 0.2–0.3. The results of the numerical calculation of equation (11), (16) (solid line), as well as the phenomenological dependence of equation (A.5) (dashed line) and the ϵ^2-function for the ideal gapless semiconductor (dots), are given in figure 2. Comparison of the solid and dotted lines in figure 2 for the region of small ϵ shows that we can treat the region $|E|/\Delta\varepsilon_g \leqslant 0.15$ as the effective gap, caused by the inhomogeneity of the composition. One can see also that the phenomenological approximation, given in the

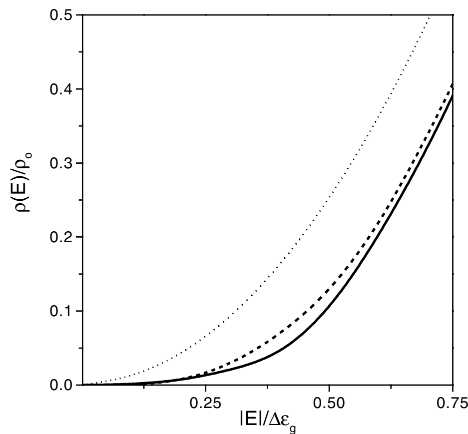

Figure 2. The energy dependence of the dimensionless density of states, determined by equation (11) and equation (16) (solid line), and by (A.5) (dashed line), and the ϵ^2-function for the ideal gapless semiconductor (dots).

appendix, leads to results close to those obtained within the microscopic Green's function investigation for the long-range case.

We mention that the expressions for $\rho(E)/\rho_0$ were obtained here for the case where the inequality

$$4m^* l_c^2\, \Delta\varepsilon_g \gg 1 \tag{18}$$

is valid. This inequality means that the deviations from the linear path, equation (15), at $\epsilon \simeq 1$ are small. The dependence $\rho(E)$ is an even one because it is determined by contributions to the density of states of the random domains with direct and inverse band structure, which are equal in volume.

4. The short-range case

In the case where the condition of smallness of equation (15) is no longer valid and long times are essential for the calculation of the path integral (this situation is realized for small l_c and non-zero values of $|E|$), one should use the self-consistent approximation [11] for the calculation of $g_t(\boldsymbol{R})$. Within this approximation we obtain the next equation for $g_t(\boldsymbol{R})$:

$$\left(\mathrm{i}\,\frac{\partial}{\partial t} + \frac{\nabla_{\boldsymbol{R}}^2}{2m^*}\right) g_t(\boldsymbol{R}) + \mathrm{i}E^2 \int_0^t \mathrm{d}t' \int \mathrm{d}\boldsymbol{R}'\, W(|\boldsymbol{R}-\boldsymbol{R}'|) G^{(3)}(\boldsymbol{R}, t|\boldsymbol{R}', t') = \delta(\boldsymbol{R})\delta(t). \tag{19}$$

Here the three-point Green's function $G^{(3)}(\boldsymbol{R}, t|\boldsymbol{R}', t')$ is determined by the factor $g_{t-t'}(\boldsymbol{R} - \boldsymbol{R}')g_{t'}(\boldsymbol{R}')$. By carrying out the Fourier transformation over time and space variables, we get the Green's function from equation (19):

$$g_E(\boldsymbol{k}) = \left[\frac{\boldsymbol{k}^2}{2m} - \frac{E^2}{\Delta\epsilon_g} + M_E(\boldsymbol{k})\right]^{-1}. \tag{20}$$

Here the mass operator $M_E(\boldsymbol{k})$ is determined by the integral equation

$$M_E(\boldsymbol{k}) = E^2 \int \frac{\mathrm{d}\boldsymbol{k}'}{(2\pi)^3}\, W(|\boldsymbol{k}+\boldsymbol{k}'|) g_E(\boldsymbol{k}') \tag{21}$$

($W(|\boldsymbol{k}|)$ is the Fourier shape function of the Gaussian correlator).

The density of states is determined through equation (20) by the relation

$$\rho(E)/\rho_0 = \frac{2}{\pi}\,\mathrm{Re} \int \frac{\mathrm{d}\boldsymbol{k}}{(2\pi)^3} \left(\epsilon + \frac{\boldsymbol{k}^2}{2m^*\,\Delta\varepsilon_g\,\epsilon}\right) g_E(\boldsymbol{k}). \tag{22}$$

The self-consistent approximation corresponds to the Dyson equation with the mass operator written in the Born approximation. In this approach, we use the free Green's function for the calculation of the right-hand side of equation (21). The mass operator that determines equation (20) is given by the equation

$$M_E(\boldsymbol{k}) \simeq \Delta\varepsilon_g\, \frac{b\epsilon^2}{16}\left(1 + \mathrm{i}\frac{\epsilon}{2}\sqrt{\frac{b}{\pi}}\right). \tag{23}$$

This equation is obtained for the conditions where the inequality inverse to equation (18) holds. Here $b \equiv m^* l_c^2\, \Delta\varepsilon_g \ll 1$. Substitution of these expressions into equation (22) gives the dependence of $\rho(E)/\rho_0$, presented in figure 3. For $b \to 0$ we get the curve for ϵ^2, corresponding to the ideal gapless semiconductor. However, at $b > 0$ this dependence differs considerably from the ϵ^2-curve. It should be noted that the inhomogeneity-induced gap for $b = 0.2$–0.4 is of the same order of magnitude as for the long-range case.

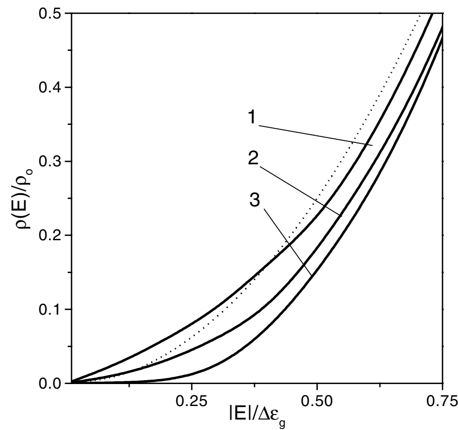

Figure 3. The energy dependence $\rho(E)/\rho_0$ for $b = 0.05$ (1), $b = 0.1$ (2), and $b = 0.2$ (3), and the function ϵ^2 for the ideal gapless semiconductor (dotted line).

5. Conclusions

The energy dependences of the density of states, presented in figures 2 and 3, are changed significantly in comparison with those for the case of the ideal homogeneous alloy with $\rho(\epsilon) \sim \epsilon^2$. The form of these modifications in the region $|E|/\Delta\varepsilon_g \leqslant 0.15$ can be treated as the effective gap, caused by the inhomogeneity of the composition. We have also demonstrated that these modifications themselves differ, showing a transition between the cases for short-range and long-range inhomogeneities. The energies of the gap that appears due to the non-uniformity of the alloy are the same in the transition region between these two limit cases (i.e. at $\Delta\varepsilon_g \simeq (4m^* l_c^2)^{-1}$). We mention also the other approximations used for the calculation of the Green's functions, equation (16) and equation (20), averaged over the non-uniformity of the composition. Consideration of the case of a plane valence band permits us both to reduce the matrix equation for the Green's function, equation (1), to a scalar one, and to neglect the additional states localized on the heterojunctions with zero gap (because the radius of these states tends to infinity for the case of a plane valence band [12]). The use of the 'virtual-crystal' model for the description of the smooth non-uniformities of the crystal does not take into consideration the broadening of the electron states due to scattering on the atomic-scale inhomogeneities. This broadening (which is responsible for the 'alloy' scattering of carriers [13]) is small for de Broglie length greater than the lattice constant. Therefore it can be neglected for the values of the crystal non-uniformity given below.

There have been no careful experimental studies of the appearance of the gap in gapless semiconductors corresponding to control of the inhomogeneity parameters $\Delta\varepsilon_g$ and l_c. The typical values $\mathrm{d}\epsilon_g/\mathrm{d}x = 0.5$ eV and $\overline{\Delta x} = 10^{-3}$ lead to $\Delta\varepsilon_g \simeq 2.5$ meV; i.e. the characteristic scale of the gap in the density-of-states curve is of meV order. The transition between the long-range and short-range cases corresponds to a value of l_c of the order of $s\hbar/\sqrt{2}\,\Delta\epsilon_g \simeq 0.12\ \mu$m (we use $s \simeq 6.7\times10^7$ cm s^{-1}). This gap can be observed on the edge of the 'fundamental' sub-millimetre absorption (see the appendix). This gives a method for estimating the correlation length.

The energy dependence $\rho(E)$ can be determined also from the temperature dependence of the electron–hole pair concentration in the intrinsic non-uniform gapless semiconductor. These concentrations are determined through ordinary statistical formulae [14]. They can be

measured from studies of the Hall effect or other kinetic effects. Besides the modification of the high-frequency and static effects or the non-uniform gapless semiconductor, the character of the fluctuations can also change ($1/f$ noise can arise for the case of long-range inhomogeneities).

Appendix

In the case of extremely long-range inhomogeneities we can obtain the $\rho(E)$ dependence by averaging the density of states for the narrow-gap semiconductor over $\epsilon_g(\boldsymbol{r})$ (the average of $\epsilon_g(\boldsymbol{r})$ in this case is zero). This approach also enables us to calculate the interband absorption coefficient, averaged over the inhomogeneities. The density of states, $\rho(E)$, and the interband absorption coefficient, $\alpha(\omega)$, for the homogeneous semiconductor with the gap width ϵ_g are given by well-known expressions:

$$\rho(E) = \frac{|E|}{\pi^2(\hbar s)^3}\sqrt{E^2 - \epsilon_g^2} \tag{A.1}$$

$$\alpha(\omega) = \frac{e^2}{3\hbar^2 c n_\omega s}\sqrt{(\hbar\omega)^2 - \epsilon_g^2}\left[1 + \frac{1}{2}\left(\frac{\epsilon_g}{\hbar\omega}\right)^2\right]. \tag{A.2}$$

Here c is the light velocity, n_ω is the refractive index. In order to calculate the density of states $\langle\rho(E)\rangle$, as well as the absorption coefficient $\langle\alpha(\omega)\rangle$ for the gapless alloy with spatial inhomogeneities of composition, we substitute for ϵ_g in equation (A.1) and equation (A.2) with $\Delta\varepsilon_g\,\delta(\boldsymbol{r})/2$ (see equation (2)) and take the average over the inhomogeneities of the alloy $\delta(\boldsymbol{r})$. Using the dimensionless energy ϵ and the frequency $\Omega = \hbar\omega/\Delta\epsilon_g$, we rewrite the initial expressions in the forms

$$\langle\rho(E)\rangle/\rho_0 = \epsilon^2\left\langle\sqrt{1 - \left(\frac{\delta(\boldsymbol{r})}{2\epsilon}\right)^2}\right\rangle \tag{A.3}$$

$$\langle\alpha(\omega)\rangle/\overline{\alpha} = \Omega\left\langle\sqrt{1 - (\delta(\boldsymbol{r})/2\Omega)^2}\left[1 + \frac{1}{2}\left(\frac{\delta_r}{2\Omega}\right)^2\right]\right\rangle \tag{A.4}$$

where ρ_0 is introduced as in equation (16), and $\overline{\alpha} = e^2\,\Delta\varepsilon_g/(3\hbar^2 c n_\omega s)$ determines the absorption coefficient for the ideal gapless semiconductor at $\hbar\omega = \Delta\varepsilon_g$.

After Fourier transforming the functions $\sqrt{1-x^2}$ and $\sqrt{1-x^2}(1+x^2/2)$, and using the expression $\langle\exp(\mathrm{i}K\delta_r)\rangle = \exp(-K^2/2)$ for the average of the random exponent (see e.g. [14]), we can rewrite (A.3) and (A.4) as

$$\frac{\langle\rho(E)\rangle}{\rho_0} = \epsilon^3\sqrt{\frac{2}{\pi}}\int_{-1}^{1}\mathrm{d}x\;\mathrm{e}^{-2(\epsilon x)^2}\sqrt{1-x^2} \tag{A.5}$$

$$\frac{\langle\alpha(\omega)\rangle}{\overline{\alpha}} = \Omega^2\sqrt{\frac{2}{\pi}}\int_{-1}^{1}\mathrm{d}x\;\mathrm{e}^{-2(\Omega x)^2}\sqrt{1-x^2}\left[1 + \frac{x^2}{2}\right]. \tag{A.6}$$

The numerical integration of these expressions leads to the results presented in figure 2 (dashed line) and figure A1. The asymptotes for $\langle\rho(E)\rangle/\rho_0$ for the cases where $\epsilon \gg 1$ and $\epsilon \ll 1$ are given by equation (17). The corresponding asymptotes for the absorption coefficient are

$$\frac{\langle\alpha(\omega)\rangle}{\overline{\alpha}} = \begin{cases} \dfrac{9}{8}\sqrt{\dfrac{\pi}{2}}\,\Omega^2 & \Omega \ll 1 \\ \Omega & \Omega \gg 1. \end{cases} \tag{A.7}$$

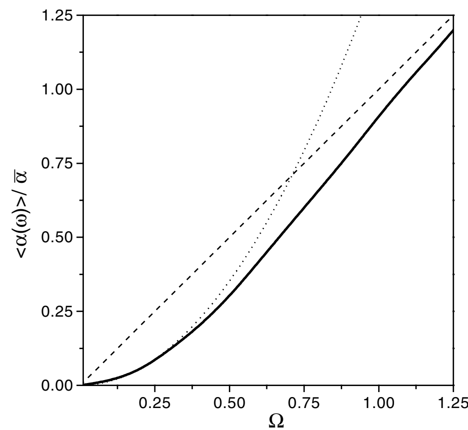

Figure A1. The absorption coefficient $\langle\alpha(\omega)\rangle/\overline{\alpha}$ calculated through equation (A.6) (solid line) and the absorption coefficient for the ideal gapless semiconductor (dashed line).

As one can see, the high-frequency limit corresponds to the absorption coefficient for the ideal gapless semiconductor. The scale of the range of frequencies where the deviation from the linear spectrum is substantial can be of the order of several meV (see section 5 and figure 1). Therefore these deviations can be studied experimentally using far-IR measurements.

References

[1] Dornhaus R, Nimtz G and Schlicht B 1983 *Narrow Gap Semiconductors (Springer Tracts in Modern Physics vol 98)* (Berlin: Springer)
[2] Tsidilkovskii I M 1992 *Usp. Fiz. Nauk* **162** 63
[3] Muller M V and Sher A 1999 *Appl. Phys. Lett.* **74** 2343
[4] Plekhanov V G 1998 *Rep. Prog. Phys.* **61** 1045
[5] Chen A B and Sher A 1995 *Semiconductor Alloys* (New York: Plenum)
[6] Bir G L and Pikus G E 1975 *Symmetry and Strain-Induced Effects in Semiconductors* (New York: Wiley)
[7] Feynman R H and Hibbs A R 1965 *Quantum Mechanics and Path Integrals* (New York: McGraw-Hill)
[8] Economou E N 1983 *Green's Function in Quantum Physics* (Berlin: Springer)
[9] Bonch-Bruevich V L, Zviagin I P, Keiper R, Mironov A G, Enderlein R and Esser B 1981 *Electronic Theory of Disordered Semiconductors* (Moscow: Nauka) (in Russian)
[10] Van Mieghen P 1992 *Rev. Mod. Phys.* **64** 755
[11] Freed K F 1970 *J. Phys. Chem. Solids* **55** 3910
[12] Pankratov O A, Pakhomov S V and Volkov B A 1987 *Solid State Commun.* **61** 93
[13] Marshak A H and van Vlient C M 1984 *Proc. IEEE* **72** 5
[14] Blakemore J S 1962 *Semiconductor Statistics* (Oxford: Pergamon)